Eur. J. Biochem. **267**, 2588–2598 (2000) © FEBS 2000

Characterization of the early steps of OE17 precursor transport by the thylakoid ΔpH/Tat machinery

Siegfried M. Musser* and Steven M. Theg

Section of Plant Biology, University of California, Davis, USA

In order to probe the structure and protein translocation function of the thylakoid Tat machinery, a 25-residue C-terminal extension containing a 13-residue *in vivo* biotinylation tag and a 6× His tag was added to a mutant precursor of the 17-kDa subunit of the oxygen-evolving complex to form pOE17(C)-BioHis. When avidin was attached to biotinylated precursor *in situ*, the precursor–avidin complex was neither imported nor did it form a membrane-spanning translocation intermediate. It did, however, competitively inhibit the translocation of unbiotinylated precursor with an apparent K_I unaffected by avidin. It is shown that the precursor protein achieves a stable folded structure upon dilution from urea, suggesting that the avidin-induced inhibition of transport results from a folding-induced proximity of N-terminal and C-terminal domains. It is further demonstrated that the majority of precursor rapidly binds to the thylakoid membrane, remaining import competent and yet undissociable by high salt or high pH treatment at ice temperature. The membrane binding event is unaffected by avidin. Import kinetics reveal that nonproton motive force-driven transport steps make up a major fraction of the transport time. These observations suggest that the N-terminal presequence on the avidin-bound precursor is available for membrane binding and initial recognition by the transport machinery, but the attached avidin signals the machinery that the precursor is an incorrectly configured substrate and thus import is aborted. Consequently, the ΔpH/Tat machinery's proofreading mechanism must operate after precursor recognition but before the committed step in transport.

Keywords: biotinylation; ΔpH/Tat machinery; protein translocation; proton motive force; thylakoid biogenesis.

Precursor proteins destined for the thylakoid lumen are transported across the thylakoid membrane by one of two translocation machineries, the cpSec machinery or the cpTat machinery. Both of these translocation machineries have now been shown to have bacterial ancestry, and are denoted the Sec and Tat machineries, respectively, in *Escherichia coli* [1–5]. The N-terminal targeting sequences for Sec and Tat precursors are very similar, the major difference being the presence of a RRXFKL consensus motif in precursors destined for twin arginine translocation (Tat) machinery transport [5–8]. For the well-characterized bacterial Sec machinery, SecY and SecE form the minimal pore-forming unit; ATP hydrolysis by SecA is essential for transport, although a proton motive force (PMF) improves transport rate and energetic efficiency [9–14]. SecA, SecY and SecE protein homologs exist in higher plant plastids [15–17]. From thylakoid membrane transport studies, the Tat machinery is recognized as being unique among protein translocating machineries in that there is no nucleotide triphosphate requirement for transport; rather, transport is driven by the PMF alone [18–20]. The membrane ΔpH is the dominant contributor to the PMF in thylakoids, and, in fact, collapse of the electric field gradient ($\Delta\Psi$) across the thylakoid membrane has no measurable effect on Tat transport efficiency [20]. Accordingly, an alternate (and original) nomenclature for the thylakoid Tat machinery is the ΔpH-dependent machinery.

Identification of the maize protein Hcf106 as the first component of the cpTat machinery [21] led to the rapid identification of the *E. coli* homologs TatA, TatB and TatE and the *tatABCD* operon [3–5]. Tha4, a homolog of Hcf106, has been identified in plants, and homologs of TatC have been identified in algae and *Arabidopsis thaliana* [22,23]. While components of the Tat machinery have thus been identified genetically in algae, plants and bacteria, no precursor protein has yet been demonstrated to interact directly with any of the encoded proteins by cross-linking studies. This has not been due to lack of effort, but rather is a consequence of the unexpectedly different functional characteristics of the Tat translocation pathway. The proven method for chemically identifying elements of protein translocation machineries, such as those found in the endoplasmic reticulum and mitochondrial membranes in addition to the Sec machineries mentioned above, is to form a membrane-spanning translocation intermediate by attaching a large, unfoldable domain at the C-terminus of a precursor protein that halts the transport process during transport across the membrane because it is too large to fit through the translocation machinery pore [24–28]. The finding that tightly folded bovine pancreatic trypsin inhibitor (BPTI) and dihydrofolate reductase (DHFR), 6.5 and 12 kDa proteins, respectively, are transported through the cpTat machinery

Correspondence to: S. M. Theg, Division of Biological Sciences, Section of Plant Biology, University of California, One Shields Avenue, Davis, CA 95616, USA. Fax: 1 530 752 5410, Tel.: 1 530 752 0624, E-mail: smtheg@ucdavis.edu

Abbreviations: BPTI, bovine pancreatic trypsin inhibitor; DHFR, dihydrofolate reductase; IPTG, isopropyl thio-β-D-galactoside; LTD, lumenal targeting domain; MPB, 3-(*N*-maleimidylpropionyl)biocytin; PMF, proton motive force; pOE17 and pOE23, precursors for the 17 and 23 kDa subunits of the oxygen evolving complex; PtdCho, phosphatidyl choline; STD, stromal targeting domain.

**Present address*: Department of Biochemistry, MS 009, Brandeis University, Waltham, MA 02454, USA

(Received 17 September 1999, revised 22 December 1999, accepted 2 March 2000)

[29,30] is understood in light of the apparent fact that the *E. coli* Tat machinery transports a multitude of redox-cofactor proteins in a fully assembled configuration [4,7,31–33]. Thus, unlike the Sec machinery, which transports proteins in a linear fashion from N-terminus to C-terminus, the present picture is that the Tat machinery transports fully folded and assembled proteins.

This study was initiated in order to further explore whether a translocation intermediate could be formed in the thylakoid membrane by attaching a large (60 kDa) avidin moiety near the C-terminus of pOE17, a protein transported by the cpTat machinery. A translocation intermediate would allow identification of components of the machinery through cross-linking experiments, whereas passage of such a construct through the cpTat machinery would allow further definition of the 'pore-size' of the machinery. In hindsight, the latter scenario is the expected result as trimethylamine N-oxide reductase and hydrogenase 2, protein complexes ≥ 90 kDa, are transported by the *E. coli* Tat machinery after insertion of their redox cofactors and after achieving their native tertiary fold [31,33]. It was thus surprising to find that the observed result was neither of these two possibilities: the precursor–avidin constructs were not transported by the cpTat machinery and yet did not demonstrate the suicide-inhibitor properties expected of membrane-spanning translocation intermediates. We note that Asai and co-workers [34] formed a translocation intermediate with biotinylated pOE23, another substrate for the cpTat machinery, in the presence of avidin. In contrast, in the work reported here on pOE17, it was found that, whereas the precursor–avidin constructs bound tightly to thylakoid membranes, such binding was not to the 'pore' of the translocation machinery but elsewhere on the membrane surface. The precursor's membrane-binding characteristics and the kinetics of import support a model of translocation wherein the precursor first binds to the membrane and then diffuses along the membrane surface to the import machinery.

MATERIALS AND METHODS

Construction of pOE17(C)-BioHis expression vector

The precursor protein utilized in thylakoid import assays consisted of the maize pOE17 protein in which the C-terminal residue had been mutated from glycine to cysteine followed by a 25-amino acid extension (IDGRLVEIFEAMKMELRGSHHHHHH) that includes an *in vivo* biotinylation tag [35] and a 6 × His-tag for purification by Ni-nitriloacetic acid chemistry. This precursor construct, termed pOE17(C)-BioHis, is encoded by the plasmid pSMM2 which was constructed as follows. The pOE17 gene was amplified from pET-prOE17$G_{217}\Delta$C [30] by PCR using primers 5′-TGCCACCATACCCACGCCGAAACAA-3′ and 5′-GACGACCATCGATACATAGCTTAGCGAGAACAtrichloroacetic acid-3′. The 0.9-kb PCR product was digested with *Xba*I–*Cla*I and ligated to the large fragment of prOE23Flag (gift of K. Keegstra, Michigan State University, East Lansing, USA) digested with the same two enzymes to yield pSMM1. The prOE23Flag plasmid consists of a modified pET-3c vector (Novagen) termed pETH3c in which the two *Eco*RV sites were first removed by *Eco*RV–*Eco*RI digestion, 5′→3′ fill-in, and blunt-end ligation; *Eco*RV and *Bgl*II sites were then introduced by insertion of 5′-Atrichloroacetic acidGATCTGAT-3′ within the *Bam*HI site (GGAT-insert-CC). The prOE23Flag plasmid was formed by inserting the pea pOE23 gene with a FLAG epitope (IDYKDDDDKL) at the C-terminus into the *Nde*I–*Eco*RV-digested pETH3c. As a *Cla*I site separates the pOE23 gene and the FLAG epitope in prOE23Flag, pSMM1 encodes pOE17 with a FLAG epitope at its C-terminus. The 94 bp primer 5′-TATGTATCGATGGTCGTCTGGTTGAAATATTCGAAGCTATGAAAATGGAACTGCGTGGCTCCCACCAtrichloroacetic acidCCATCACCATTAGGATAtrichloroacetic acidCGCA-3′ was amplified by PCR using primers 5′-TATGTATCGATGGTCGTCTG-3′ and 5′-TGCGTGATATCCTAATGGTG-3′. The PCR product was digested with *Cla*I–*Eco*RV, and the resulting 77-bp segment was ligated to the large fragment of pSMM1 digested with the same enzymes to yield pSMM2, thus replacing the FLAG epitope with the BioHis extension. The correct amino acid sequence was confirmed by sequencing the DNA insert.

Overexpression of pOE17(C)-BioHis

The precursor pOE17(C)-BioHis was overexpressed from pSMM2 in *E. coli* strain BL21(DE3) [F^- *ompT hsd*S_B (r_B^- m_B^-) *gal dcm* (DE3)]. For radioactive protein, cells were grown at 37 °C in M9 minimal media [36] with 0.5% tryptone to $A_{600} \approx 0.6$–0.8, centrifuged, and resuspended at $A_{600} \approx 2.0$ in 10 mL M9 media in the presence of 0.5 mCi·mL^{-1} ^{3}H-leucine (NEN-DuPont), 1 mM isopropyl thio-β-D-galactoside (IPTG) and 0.2 mM rifampacin. Total induction time was 4–6 h. Nonradioactive protein was obtained from cells grown to $A_{600} \approx 0.6$–0.8 in M9 or Luria-Bertani [36] media and then induced with 1 mM IPTG as above. To obtain *in vivo* biotinylated protein, the biotin ligase (BirA)-expressing plasmid pCY216 (gift of John Cronan, University of Illinois, Urbana, USA) [37] was induced using 0.5% arabinose at least 15 min before IPTG induction. The compatible pSMM2 and pCY216 plasmids were maintained independently using 100 μg·mL^{-1} carbenicillin and 50 μg·mL^{-1} chloramphenicol, respectively.

Purification of pOE17(C)-BioHis

Radioactive overexpressed protein was purified by solubilization of ≈ 100 mg cells with 2.5 mL buffer A (8 M urea, 100 mM sodium phosphate, 50 mM sodium citrate, pH 8.0), 50 μL 50 mM phenylmethane sulfonyl fluoride in isopropanol, 2.5 μL 20 mg·mL^{-1} apoprotinin, 2.5 μL 1 mg·mL^{-1} leupeptin, 1.8 μL 2-mercaptoethanol, 250 μL 10% Triton X-100 and 50 μL 1 M imidazole, pH 8.0. After stirring for 10 min, ≈ 1 mg DNase I was added. The solubilization was continued with stirring for a total of 1 h at room temperature. After centrifugation for 10 min at 10 000 ***g***, the supernatant was mixed with 0.8 mL 50% Ni-nitriloacetic acid (Qiagen) that had been equilibrated with buffer A + 20 mM imidazole. The solubilized protein was stirred with the resin for 45 min at room temperature. The slurry was then poured into a column, and the resin was washed with a mixture of 3.15 mL buffer A, 0.5 mL 10% Triton X-100, 1.25 mL 4 M NaCl and 100 μL 1 M imidazole, pH 8.0. After washing with 5 mL buffer A, pH 6.5, the pH was lowered to 4.5 to elute the protein. The first two milliliters of the eluant was precipitated with an equal volume of cold 30% trichloroacetic acid on ice for 30 min. The pellet that resulted from microcentrifugation for 15 min was solubilized in 50 μL buffer D (8 M urea, 200 mM sodium phosphate pH 7.0) and stored at −80 °C. The concentration of this pOE17(C)-BioHis stock solution was determined by the BCA assay (Pierce) using BSA as the standard and varied from ≈ 30 to 100 μM. Radioactivity was typically determined to be ≈ 0.5–1 × 10^{17} d.p.m.·mol^{-1}. Nonradioactive protein was

purified in a similar manner appropriately scaled to accommodate ≈ 10-fold more cells.

In vivo biotinylated pOE17(C)-BioHis was further purified over monomeric avidin resin (Pierce) following the manufacturer's advice as follows. The high-affinity biotin binding sites on 0.5 mL resin were first blocked by successive addition of 8 mL urea/NaCl/P_i (0.4 M urea, 100 mM sodium phosphate, 150 mM NaCl, pH 7.0), 6 mL BE buffer (0.4 M urea, 100 mM sodium phosphate, 150 mM NaCl, 2 mM D-biotin, pH 7.0), 12 mL 100 mM glycine, pH 2.8 and another 8 mL urea/NaCl/P_i. The precursor stock obtained from the Ni-nitriloacetic acid column was diluted 20-fold with 100 mM sodium phosphate, 150 mM NaCl, pH 7.0 and applied to the monomeric avidin column. The column was washed with 8 mL urea/NaCl/P_i and the protein was eluted with BE buffer. Fractions containing protein were combined, precipitated with trichloroacetic acid as above and solubilized with 100 μL buffer D.

3-(*N*-Maleimidylpropionyl)biocytin Labeling

The pOE17(C)-BioHis precursor was labeled with the sulfhydryl specific biotinylating reagent 3-(*N*-maleimidylpropionyl)biocytin (MPB; Molecular Probes). To insure that all cysteines were reduced, precursor stock was incubated with ≈ 100-fold excess of 2-mercaptoethanol for 10 min. The protein was precipitated with cold 30% trichloroacetic acid on ice and the pellet obtained upon microcentrifugation was resuspended in buffer D. Precursor was typically incubated with ≈ 50-fold molar excess of MPB from a dimethylsulfoxide stock for 15 min. After the reaction was quenched with a fourfold molar excess (over MPB) of 2-mercaptoethanol for 10 min, the labeled protein was precipitated with trichloroacetic acid on ice and resuspended in buffer D as described above.

Thylakoid import assays

Pea (*Pisum sativum*, Progress #9, Harris Seeds, Rochester, NY) seedlings were grown in moist vermiculite for 10–14 days at 18–24 °C under 10 h darkness and 14 h light. Chloroplasts were isolated essentially as described earlier [38,39] by grinding leaves at low speed in a blender in GB (grinding buffer: 50 mM potassium Hepes, 330 mM sorbitol, 1 mM $MgCl_2$, 1 mM $MnCl_2$, 2 mM EDTA, 0.1% BSA, pH 7.3), centrifuging the Miracloth filtered homogenate 5 min at 3000 ***g***, and purifying on a 50% Percoll gradient for 10 min at 8000 ***g***. Percoll and GB were removed by dilution with IB (import buffer: 50 mM potassium tricine, 330 mM sorbitol, 3 mM $MgCl_2$, pH 8.0) and centrifugation at 1500 ***g*** for 5 min. Thylakoids were prepared by osmotic lysis of chloroplasts [20] in 10 mM Mes, 5 mM $MgCl_2$, pH 6.5 on ice for 5 min. After adding an equal volume of 2× IB, the thylakoids were centrifuged at 1500 ***g***, washed once and resuspended in IB or one of a number of other buffers (IB2: 50 mM sodium tricine, 330 mM sorbitol, 5 mM $MgCl_2$, pH 7.8; IB3: 100 mM sodium tricine, 330 mM sorbitol, 5 mM $MgCl_2$, pH 7.8; MMT-IB: 50 mM Mops, 50 mM Mes, 50 mM Taps, 5 mM $MgCl_2$, pH 7.8). Chlorophyll concentration was determined as described previously [40]. Import reactions (60 μL) were conducted in the light emmitted from a 60-W tungsten bulb passed through an aqueous $CuSO_4$ infrared filter, and were stopped with a 10-fold excess of ice-cold IB. For thermolysin-treated samples, this IB quench contained 0.2 mg·mL^{-1} thermolysin, 5 mM $CaCl_2$ (and sometimes 10 μM CCCP) and was kept on ice in the dark for 15–20 min; protease activity was quenched by addition of 30 μL 500 mM EDTA, pH 8.0 and a further 2 min incubation on ice. Thylakoids were then reisolated by a 20-s microcentrifugation step. Samples were analyzed by SDS/PAGE, fluorography and densitometry (BioImage; Millipore).

Vesicle binding assay

Thylakoid lipid vesicles were made from a 20-mg·mL^{-1} lipid solution in IB by extrusion (15 times) through two 100-nm membranes using a handheld extruder (Avestin, Ottawa, Canada). The lipid composition was 50% digalactosyldiacylglycerol, 20% monogalactosyldiacylglycerol and 30% egg phosphatidylcholine (PtdCho). Digalactosyldiacylglycerol and monogalactosyldiacylglycerol were from Lipid Products (Red Hill, UK) and PtdCho was from Avanti Polar Lipids (Alabaster, Alabama, USA). After incubating 40 μL vesicles with 5 μL 2 μM pOE17(C)-BioHis, the solution was loaded onto a 0.7 × 8 cm G-100–120 size-exclusion column (Sigma). Fraction collection (250 μL each) was begun immediately after loading using IB as the running buffer.

Other

Avidin was purchased as NeutrAvidin from Molecular Probes. Western blots were blocked with 1% gelatin for 30 min, probed with 1 : 6000 dilution of strepavidin–alkaline phosphatase conjugate (Bio-Rad) in 1% gelatin for 10–20 min, visualized using Vistra ECF reagent (Amersham) and recorded on a STORM 860 PhosphoImager (Molecular Dynamics). Fluorescence spectra were obtained using an SLM AMINCO-Bowman Series 2 Luminescence Spectrometer; CD measurements were made on a Jasco J-600 spectropolarimeter.

RESULTS

Design and biotinylation of pOE17(C)-BioHis

The pOE17(C)-BioHis chimera was designed as a Tat machinery substrate that might potentially form a membrane-spanning translocation intermediate when complexed with avidin. Membrane-spanning translocation intermediates have found widespread use in the characterization of other translocation machineries [24,27,28], and in general is accomplished by synthesizing a precursor construct with a tightly folded C-terminal domain that can not be accomodated by the translocation machinery. Previous attempts to make such a translocation intermediate on the thylakoid Tat pathway were unsuccessful since the relatively small folded domains of BPTI (6.5 kDa) and DHFR (12 kDa) are transported by the transport machinery [29,30]. Our strategy was to attach a much larger protein, avidin (60 kDa), to the C-terminal region of OE17 through a biotin linkage, and hence directly test the idea that only relatively small proteins could be transported in folded conformations. To this end, we designed the 25-amino acid extension shown in Fig. 1A and engineered it on the C-terminal end of the maize pOE17 precursor (Materials and methods). This chimera contains a unique cysteine at the original C-terminus which can be chemically biotinylated *in vitro*. The C-terminal extension contains a 13-amino acid domain that is recognized and biotinylated at a unique lysine residue by biotin ligase *in vivo* [35], and in addition, contains a 6 × His-tag at the extreme C-terminus for ease in purification.

Overexpression and purification of pOE17(C)-BioHis as described in Materials and methods results in highly purified protein as shown in Fig. 1B. Use of the sulfhydryl specific biotinylation reagent MPB allows estimation of the *in vivo* biotinylation yield as 10–20% (Fig. 1C,D). This technique

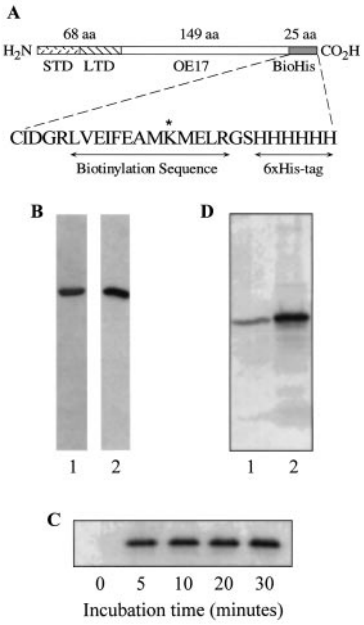

Fig. 1. Purification and biotinylation of pOE17(C)-BioHis. (A) Schematic of pOE17(C)-BioHis showing the stromal targeting domain (STD), lumenal targeting domain (LTD) and the C-terminal 25 amino acid BioHis extension on the mature domain of the maize 17 kDa subunit of the oxygen-evolving complex (OE17). (B) Typical samples of Ni-nitriloacetic acid purified pOE17(C)-BioHis: Coomassie brilliant blue stain (lane 1), fluorograph (lane 2). (C) Chemical biotinylation of purified pOE17(C)-BioHis expressed in the *absence* of biotin and biotin ligase (see Materials and methods). After ≈15 min with an ≈50-fold excess of the sulfhydryl specific reagent MPB, labeling is essentially complete as detected by Western blotting. (D) Purified pOE17(C)-BioHis expressed in the *presence* of biotin and biotin ligase (lane 1) shows a dramatic increase in biotinylation upon 15 min reaction with a 64-fold excess of MPB (lane 2). This Western blot assay provides an estimate of the *in vivo* biotinylation yield (see text).

assumes that, *in vivo*, the precursor is enzymatically biotinylated only at the lysine residue in the biotinylation sequence and MPB only reacts with the unique cysteine within pOE17(C)-BioHis. However, since the precursor is stable in low urea buffer (see below), we found it possible to obtain highly purified *in vivo* biotinylated protein through use of a second column containing monomeric avidin resin. The MPB biotinylated precursor is referred to as 'chemically biotinylated pOE17(C)-BioHis', and the *in vivo* biotinylated precursor is referred to as 'enzymatically biotinylated pOE17(C)-BioHis.'

Effect of avidin on thylakoid import

Biotinylated pOE17(C)-BioHis was imported efficiently into thylakoids. Precursor translocation was impeded by the addition of an excess of avidin if the biotin binding sites on avidin were not preblocked with free biotin (Fig. 2A). These data are expected if a translocation intermediate had formed; in such a scenario, the bulky avidin moiety prevents passage through the translocation apparatus and the precursor remains stuck in the machinery. However, radioactive, unbiotinylated precursor translocation was unimpeded in the presence of avidin and biotinylated precursor, indicating that the desired translocation intermediate was not formed (Fig. 2B). While these data can not rule out an interaction between the *in situ* generated precursor–avidin complex and the translocation machinery, they do indicate that any such interaction must be short-lived

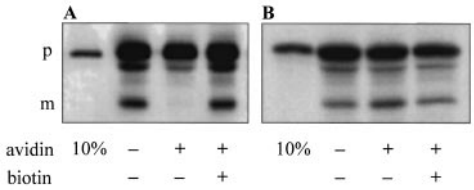

Fig. 2. Avidin prevents thylakoid import of biotinylated pOE17(C)-BioHis but does not block machinery function. Thylakoids (300 μg·mL^{-1} chlorophyll) in IB were incubated with a mixture of 100 nM ^{3}H-pOE17(C)-BioHis and 100 nM chemically biotinylated pOE17(C)-BioHis (reacted with an 50-fold excess of MPB for 15 min as shown in Fig. 1C) under illumination for 20 min. Where indicated, the avidin concentration was 4 μM and the biotin concentration was 160 μM. Thylakoid pellets were analyzed by SDS/PAGE. (A) A Western blot and thus only biotinylated protein is detected; (B) a fluorograph and thus only radioactive protein is detected. Full-length and mature-length precursor is marked by 'p' and 'm', respectively. The leftmost lane in each panel contains 10% of the total precursor mix in the reaction.

and therefore insufficient to completely block translocation of unbiotinylated precursor.

The interaction of the precursor–avidin complex with the translocation machinery was further examined by conducting thylakoid import experiments with a fixed amount of radioactive precursor and titrating in increasing amounts of nonradioactive, biotinylated precursor. In the absence of avidin, the mature radioactive protein obtained decreased as a consequence of increased competition with the nonradioactive precursor for translocation machinery binding sites. In the presence of avidin, there was a similar decrease in radioactive precursor import efficiency as the concentration of biotinylated precursor was increased (Fig. 3). Because the precursor import velocity is near maximal at the experimental precursor concentration and many turnovers occurred during the experiement, it was anticipated that in the presence of avidin there would be a steep decrease in radioactive precursor import efficiency at low concentrations of biotinylated precursor that would arise from stable blockage of the import machinery. However, in this type of competition experiment, the *plus* avidin curve was never observed below the *minus* avidin curve; rather, the pOE17(C)-BioHis inhibition of ^{3}H-pOE17(C)-BioHis import was always slightly less pronounced in the *plus* avidin titration. The data indicate, therefore, that although the precursor–avidin complex did not block transport in the manner expected for a suicide inhibitor, it did still interact with the transport machinery. The competitive nature of this interaction provides strong evidence that the receptor domains of the import machinery interact with the precursor–avidin construct in a wild-type binding mode. While the data shown in Figs 2 and 3 utilized chemically biotinylated pOE17(C)-BioHis, enzymatically biotinylated precursor yielded similar results (not shown).

Three-dimensional conformation of pOE17(C)-BioHis

The data described above revealed that a large avidin moiety near the C-terminus of pOE17(C)-BioHis prohibited transport but minimally affected the initial interaction with the translocation machinery. The precursor–avidin construct did not act as a suicide inhibitor but rather allowed transport of an avidin-free precursor. It appears, then, that after the initial interaction between transport machinery and precursor protein, the avidin-bound precursor was released. The initial precursor–transport

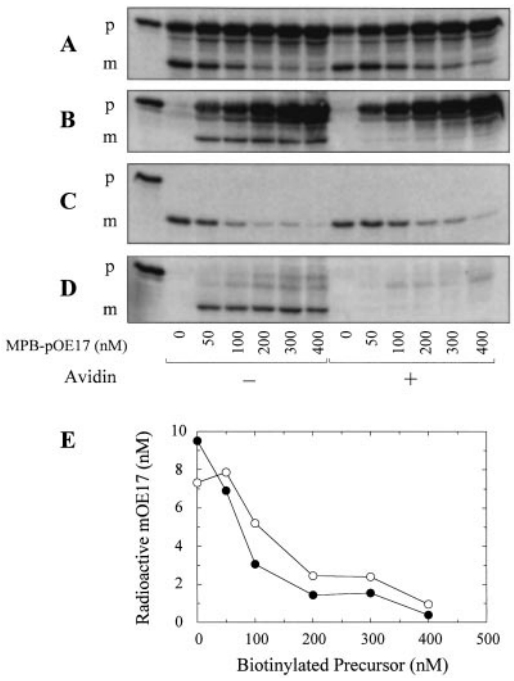

Fig. 3. Competition of chemically biotinylated pOE17(C)-BioHis with radioactive pOE17(C)-BioHis during thylakoid import. Thylakoids (300 μg·mL^{-1} chlorophyll) in IB were incubated with 100 nM ^{3}H-pOE17(C)-BioHis for 20 min under import light. MPB biotinylated precursor was included at the concentrations indicated (nM). When added, the avidin concentation was 4 μM. The leftmost lanes contain a load corresponding to 10 nM (A and C) or 50 nM (B and D) precursor. Import samples were split in half immediately upon removal from import light and quenched in IB (A and B) or thermolysin solution (C and D) as described in Materials and methods and analyzed by fluorography (A and C) and Western blotting (B and D). The amount of mature protein observed in each lane in (C) is displayed graphically in (E). These are the same preparations of precursors that were used in Fig. 2.

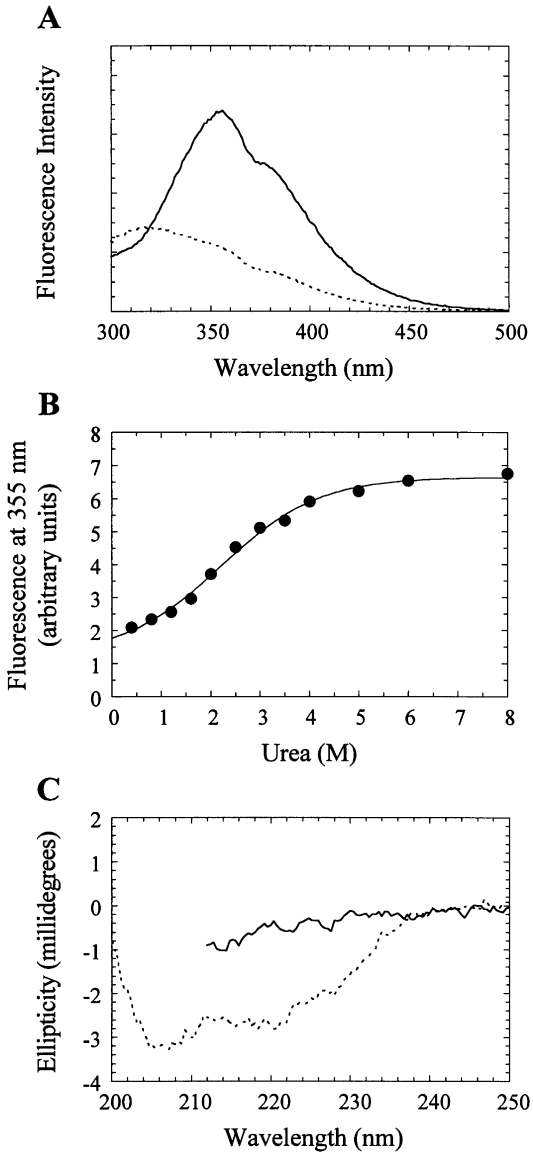

Fig. 4. Fluorescence and CD of pOE17(C)-BioHis at low and high urea concentrations. (A) Fluorescence spectra of 3.9 μM pOE17(C)-BioHis in 100 mM sodium phosphate, pH 7.0 at 0.2 M (dashed line) and 8 M (solid line) urea concentrations using an excitation wavelength of 285 nm. (B) Using fluorescence spectra obtained as in (A), the fluorescence intensity at 355 nm is plotted as a function of urea concentration. Spectra were recorded ≈ 3 min after dilution. Data were fitted using a two-state folding model (U ⇌ N) as described in the text. (C) CD spectra of 4.6 μM pOE17(C)-BioHis in 100 mM sodium phosphate, pH 7.0 at 0.2 M (dashed line) and 6 M (solid line) urea concentrations using a 0.2-mm cuvette.

machinery interaction presumably occurs primarily with the lumenal targeting domain (LTD) of the transit peptide. A subsequent transport step could potentially be perturbed if the bound avidin moiety is juxtaposed near the LTD. Such a scenario is possible if the precursor maintains a configuration in which the N-terminus and C-terminus are relatively close to each other during transport. Note that this situation is significantly different to that observed for Sec machinery translocation or transport into mitochondria, wherein substantial translocation of a precursor protein occurs before a C-terminal-folded domain affects the translocation process. To investigate this interpretation further, the conformation of the OE17 precursor was examined.

Since the pOE17(C)-BioHis construct contains a single tryptophan residue at position 139 (approximately in the middle of the OE17 mature domain), tryptophan fluorescence was used as a reporter for protein conformation. In 8 M urea, pOE17(C)-BioHis yields a tryptophan fluorescence maximum at ≈ 355 nm; this maximum shifts to ≈ 315 nm and is substantially diminished in intensity when the urea is diluted to 0.2 M (Fig. 4A). When the fluorescence intensity at 355 nm was monitored as a function of urea concentration (Fig. 4B), the data could be fitted with a model that assumes a simple two-state folding transition [41]:

$$\Delta G_{\text{fold}} = -\text{RT} \ln K_{\text{eq}} = \Delta G_{\text{fold}}^{\text{H}_2\text{O}} + m\,[\text{urea}]$$

where $K_{\text{eq}} = [\text{N}]/[\text{U}]$, N denotes the native conformation, U denotes the unfolded state and m reflects the dependence of the free energy on the denaturant concentration. In this model, $\Delta G_{\text{fold}}^{\text{H}_2\text{O}}$ is a measure of the stability of the protein in the absence of denaturant and is -6.7 ± 1.7 kJ·mol^{-1} (mean ± SD) according to three independent determinations. The midpoint of the folding transition, or $[\text{urea}]_{1/2}$, is 2.22 ± 0.03 M.

As the above fluorescence experiments provide limited information about protein conformation as a whole but rather report changes in the immediate environment of the tryptophan residue, we also measured the CD of pOE17(C)-BioHis in low and high urea buffers (Fig. 4C). The data show that there was significant secondary structure (suggestive of tertiary structure) in 0.2 M urea which was nonexistent when the urea concentration

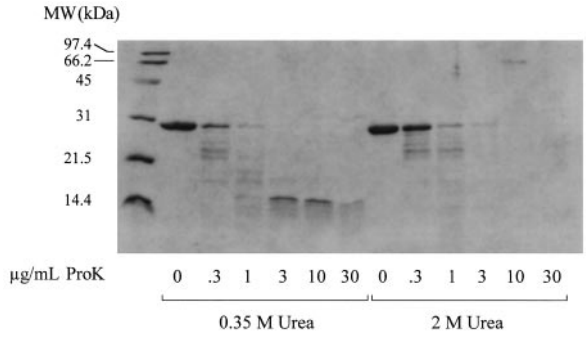

Fig. 5. Proteinase K digestion of pOE17(C)-BioHis at low and high urea concentrations. In 50 mM sodium phosphate, pH 7.0 buffer, 13.7 μM pOE17(C)-BioHis was incubated with the indicated proteinase K concentrations at low (0.35 M) or high (2 M) urea concentrations. After 15 min at room temperature, the digestions were stopped by addition of 1 μL 20 mM phenylmethane sulfonyl fluoride in isopropanol. The leftmost lane contains molecular mass standards of the indicated mass.

was 6 M. As a third independent means by which tertiary structure can be assessed, we subjected pOE17(C)-BioHis to digestion with increasing amounts of proteinase K in low (0.35 M) and high (2 M) urea buffers (Fig. 5). The data reveal an $\approx$15 kDa fragment that is resistant to intermediate concentrations of protease at low urea concentration. The fluorescence, CD and protease digestion data are all consistent with a model in which pOE17(C)-BioHis folds into a defined configuration. The configuration of the mature domain may in fact resemble the native conformation of the protein in its functional role as part of the oxygen-evolving complex, but this possibility is difficult to assess. In any case, these data provide a rationale for why the attempts described above to create a translocation intermediate with an untransportable substrate were unsuccessful; namely, a bulky avidin bound near the C-terminus may be juxtaposed near the N-terminal signal sequence. As a consequence, while the initial interaction with the translocation machinery is unaffected, the structure of the precursor–avidin complex is incompatible with a later transport step. We note that there is no evidence suggesting that the structural stability of the OE17 domain was affected by the presence of the bound avidin moiety according to the proteinase K digestion assay (data not shown).

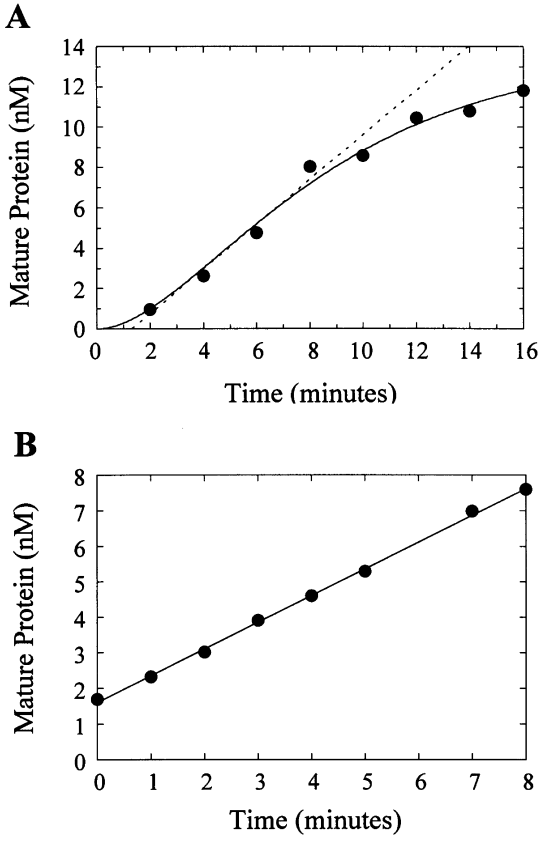

Fig. 6. Import of thylakoid-bound pOE17(C)-BioHis. (A) Aliquots (60 μL) from a 600 μL thylakoid import reaction containing 300 $\mu g \cdot mL^{-1}$ chlorophyll and 100 nM ^{3}H-pOE17(C)-BioHis in IB2 were removed at the indicated time points, treated with thermolysin and analyzed by SDS/PAGE. The solid line fit assumes an irreversible two-step first-order reaction, i.e. A $\xrightarrow{k_1}$ B $\xrightarrow{k_2}$ C, with rate constants $k_1 = 0.219\ min^{-1}$ and $k_2 = 0.221\ min^{-1}$, respectively. The dashed line passes through the point of maximum slope. (B) A 600-μL thylakoid import reaction containing 300 $\mu g \cdot mL^{-1}$ chlorophyll and 100 nM ^{3}H-pOE17(C)-BioHis in IB3 was incubated for 10 min and then microcentrifuged for 20 s. The thylakoids were resuspended in 600 μL IB3 and import was initiated by illumination. Samples were kept in the dark as much as feasible until import initiation. Aliquots (60 μL) were quenched at the indicated time points and analyzed as described for (A). Note the different abscissa scales for (A) and (B).

Membrane-bound pOE17(C)-BioHis is import competent

As Figs 2 and 3 demonstrate, a substantial fraction of the added radioactive and biotinylated precursor bound to the thylakoid membrane in the presence and absence of avidin. Three possible binding sites for the membrane-bound precursor can be envisaged: a proteinaceous element of the Tat machinery, a non-Tat protein or the membrane lipid. The fact that transport was not blocked by saturating concentrations of a nontransportable substrate complicates any interpretation wherein such precursor binds to an element of the Tat machinery. Alternatively, if the nontransportable precursor is bound elsewhere on the membrane surface, either to another protein or to the membrane surface itself, the physiological relevence of this bound precursor is not obvious – such precursor could simply be aggregated protein nonspecifically stuck to the membrane surface in an import-incompetent state. However, such nonspecific binding seemed unlikely in light of the fact that we demonstrated that the pOE17(C)-BioHis precursor is soluble upon dilution from urea, folding to a stable conformation which is import competent in reaction buffer for hours, and in addition, can be purified on Ni-nitriloacetic acid or monomeric avidin resins using buffers devoid of urea. These physical properties of pOE17(C)-BioHis indicating stability in aqueous media as a soluble protein suggested to us that it is unlikely for this precursor to nonspecifically aggregate on the thylakoid membrane. We thus investigated the import competence of membrane-bound precursor.

A time course of pOE17(C)-BioHis import wherein thylakoids and precursor were mixed and import began immediately showed biphasic kinetics (Fig. 6A), as reported previously for wild-type pOE17 and pOE23 [42,43]. To investigate the import competence of thylakoid-bound precursor, thylakoids were separated from soluble precursor by microcentrifuging the sample for 20 s. These thylakoids were then resolubilized in import medium and illuminated. Import of thylakoid-bound precursor assayed in this way (Fig. 6B) occurred at a rate comparable with normal import reactions (Fig. 6A). It should be pointed out that these experiments, while simple in principle,

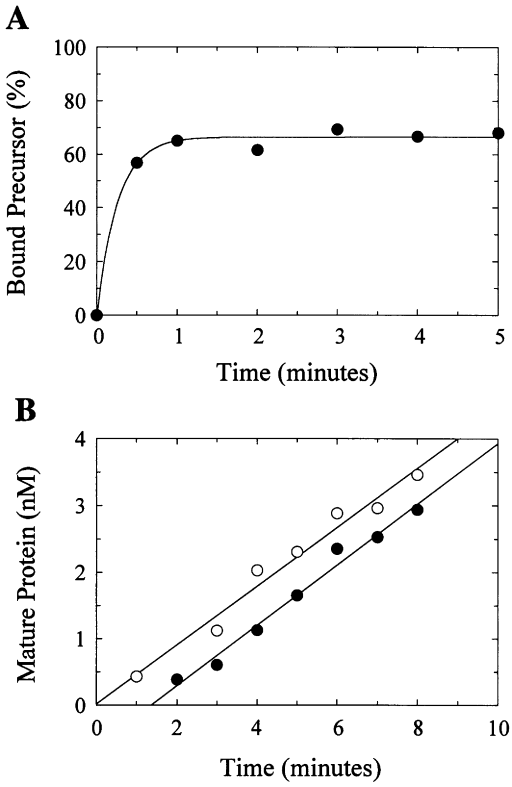

Fig. 7. Thylakoid membrane binding is responsible for the initial lag in import time course. (A) A 600-μL reaction incubation containing 300 μg·mL^{-1} chlorophyll and 100 nM ^{3}H-pOE17(C)-BioHis in MMT-IB was incubated in the dark at room temperature. Aliquots (60 μL) were removed at the indicated time points, quenched by 10-fold dilution into IB and immediately microcentrifuged for 20 s. (B) Thylakoid import reactions (600 μL) containing 300 μg·mL^{-1} chlorophyll in MMT-IB were incubated in the dark for 5 min without precursor (●) or with 100 nM ^{3}H-pOE17(C)-BioHis (○). An equivalent amount of precursor was added to the 'no precursor' sample and import was initiated immediately. Import was initiated in the remaining sample by transfer to the light. Aliquots (60 μL) were quenched at the indicated time points and analyzed as in Fig. 6.

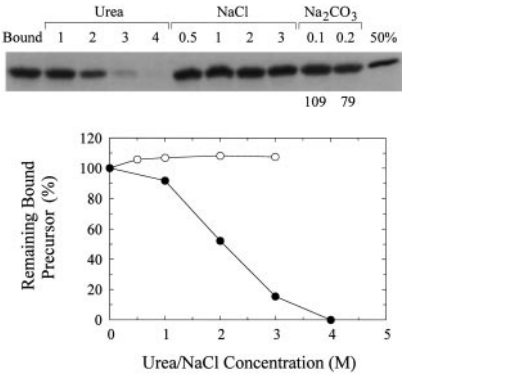

Fig. 8. Dissociation of thylakoid-bound pOE17(C)-BioHis by various chemical reagents. A 720-μL reaction mix containing 300 μg·mL^{-1} chlorophyll and 100 nM ^{3}H-pOE17(C)-BioHis in MMT-IB was incubated in the dark at room temperature for 5 min. Aliquots (60 μL) were removed and simultaneously microcentrifuged for 20 s. Thylakoids were resuspended in MMT-IB containing the indicated concentration (M) of chemical reagent. After incubating on ice in the dark for 30 min, thylakoids were microcentrifuged for 20 s and analyzed. The leftmost lane contains precursor bound after incubation with just buffer and amounts to 82% of the added precursor. The rightmost lane represents 50% of the added precursor. The amount of bound precursor surviving the urea (●) and NaCl (○) treaments is shown graphically, calibrated to the left-hand lane (100%). The numbers below the Na_2CO_3 (pH 10.9) lanes denote the percent of bound precursor surviving the treatment.

are difficult in practice because all light must be excluded while thylakoids and precursor are incubated, centrifuged and resuspended. Light leaking into the sample during these experimental manipulations is undoubtedly responsible for the zero timepoint in Fig. 6B yielding a nonzero ordinate as other experiments revealed that no import occurred if the sample was simply left in the dark for a similar period (data not shown). Nonetheless, these data indicate that thylakoid-bound precursor remains import competent and suggest the possibility that the stable, thylakoid-bound state is a pathway intermediate.

Rate of pOE17(C)-BioHis association with the thylakoid membrane

We then investigated whether the thylakoid association of pOE17(C)-BioHis occurs on a timescale consistent with this process being an early step in the transport process. To address this question, thylakoids and precursor were mixed in the dark and aliquots were removed after select time intervals, diluted 10-fold with ice-cold import buffer and immediately microcentrifuged for 20 s. In this manner, it was found that the precursor bound to the thylakoid membrane with a half-time of < 1 min (Fig. 7A). A more accurate binding rate is unattainable by this method because of the time required for the initial hand mixing, quenching by dilution and centrifugation of the aliquots. In a typical experiment, 60–80% of the added precursor maximally bound to the thylakoids. When precursor and thylakoids were pre-incubated in the dark for 5 min, allowing membrane binding to reach completion before initiating import, the import time course was linear and a linear regression fit passed through the origin (Fig. 7B). A control time course with no pre-incubation period showed a lag of ≈ 1 min before mature protein first appeared, in agreement with published data [42,43] and that in Fig. 6A. These data demonstrate that a kinetically slow step of the transport process occurs before the energy requiring transport step(s).

Dissociation of pOE17(C)-BioHis from the thylakoid membrane

The nature of the precursor's interaction with the membrane was addressed using various chemical reagents. After the precursor was pre-incubated with thylakoids in the dark for 5 min and the samples were microcentrifuged, the thylakoids were resuspended and incubated on ice in the dark for 30 min with one of a number of chemical reagents (Fig. 8). The data indicate that the precursor–membrane interaction was not ionic as there was no precursor dissociation with up to 3 M NaCl. In addition, the precursor was not dissociated in high pH carbonate buffer, a condition that typically removes peripheral proteins [44,45]. The precursor was 100% dissociated from the membrane with 4 M urea, however.

pOE17(C)-BioHis binds to thylakoid lipid vesicles

The membrane-bound form of pOE17(C)-BioHis can interact with membrane proteins, the membrane lipid itself or a combination of both. The nature of this interaction was further explored by determining whether the precursor binds to lipid

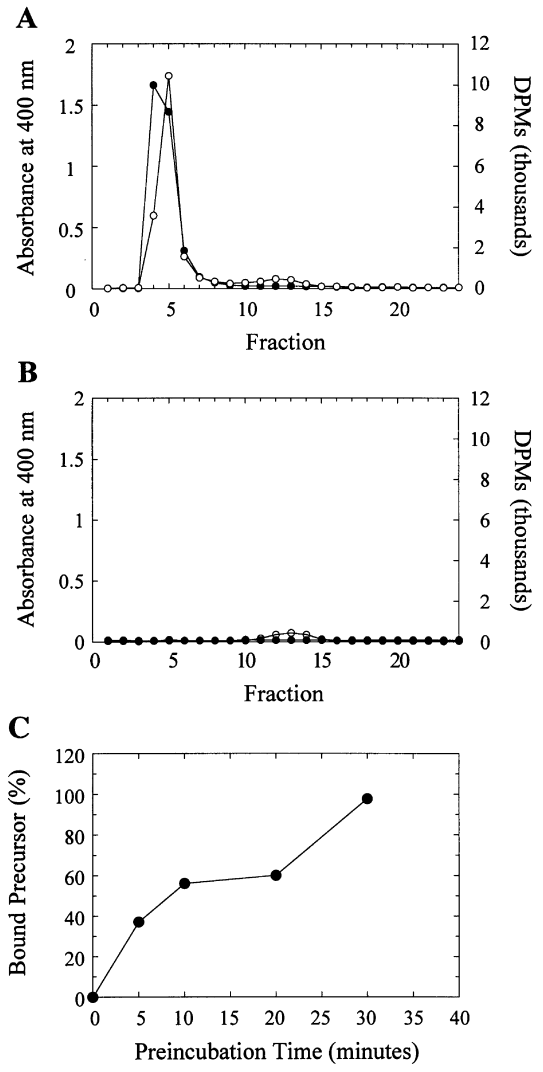

Fig. 9. pOE17(C)-BioHis binds to thylakoid lipid vesicles. Thylakoid lipid vesicles were incubated with pOE17(C)-BioHis and passed over a G-100-120 size-exclusion column as detailed in Materials and methods. (A) Vesicles + precursor; (B) vesicles alone; (C) percentage of added precursor eluting in vesicle fractions (fractions 4–6) as a function of the time precursor was incubated with vesicles before loading column. For (A) and (B), vesicle scattering was detected at 400 nm (●) and precursor radioactivity (○) was measured as disintegrations per minute (d.p.m.).

vesicles made from thylakoid lipids. Vesicles that had been incubated with precursor protein were passed over a size-exclusion column and the fractions were assayed for the presence of vesicles (by the scattering at 400 nm) and precursor (by the radioactivity). The precursor protein clearly eluted in the vesicle fractions (Fig. 9). Intriguingly, in the absence of vesicles, the majority of precursor protein never eluted from the column (Fig. 9), indicating that the precursor must interact strongly with the column matrix. An explanation for this observation is that the hydrophobic elements of the targeting sequence interact strongly with the stationary phase and this interaction was prevented when a precursor molecule was bound to a vesicle. In the presence or absence of vesicles, $\approx 10\%$ of the radioactivity eluted in later fractions (fractions 10–15); this location in the elution profile is consistent with monomeric precursor protein that had survived the column. It is noteworthy that the precursor bound to the vesicles quite slowly as a pre-incubation period of ≈ 30 min was required in order for the majority of protein to elute in the vesicle fractions (Fig. 9C). This binding rate is much slower than that observed for thylakoids (Fig. 7A) and potentially results from the different lipid composition of the vesicles compared with thylakoid membranes. The different lipid composition is necessitated by the fact that it is not possible to form pure lipid vesicles with the high concentrations of monogalactosyldiacylglycerol found in thylakoid membranes because this lipid favors the hexagonal II phase (e.g. it is a nonbilayer forming lipid) [46]. The high concentration of proteins in the thylakoid membrane and the unique topology of these membranes may also play a role in the lipid packing structure in a way that affects the precursor's binding rate. While a direct role of thylakoid proteins in the binding of precursor can not be ruled out, and, in fact, can be considered likely, these data demonstrate that pOE17(C)-BioHis binds strongly to pure lipid bilayers. However, it is possible that the precursor's kinetically slow interaction with the vesicles is nonspecific and chemically dissimilar to the rapid tight binding interaction to the thylakoid membrane.

DISCUSSION

The discovery of the maize Hcf106 protein and its bacterial homologs [21] and the subsequent flurry of work on the translocation machineries of which these proteins are part has led convincingly to the understanding that the Tat complex is truly a new and unique type of protein translocating machinery [3–5,8,47,48]. Protease digestion assays indicate that the OE23 protein is folded when presented to thylakoids for transport [49], probably remaining this way during normal transport by the Tat machinery [29]. Folded proteins are clearly transported by the Tat machinery [29,30]. The homologous *E. coli* machinery appears to be designed to recognize and transport large, folded and assembled proteins such as TMAO reductase and hydrogenase 2 ($\geq$ 90 kDa) [31,33]. The work presented here demonstrating that the OE17 protein is also folded when presented to thylakoids adds to this picture. Furthermore, it is the first set of data that addresses the three-dimensional conformation of this particular precursor protein in solution. The high purity of the pOE17(C)-BioHis protein used here, and the fact that it folds rapidly (within seconds) and spontaneously, indicates that molecular chaperones are not required for the folding process. In our hands, pOE23 appears to have a more complicated folding landscape because a pOE23-BioHis construct made and purified as for the pOE17(C)-BioHis construct rapidly aggregates and precipitates upon dilution from urea (Q. Luu, S. M. Musser and S. M. Theg, unpublished results).

The fact that our precursor–avidin complex is not transported and yet reduces the efficiency of transport of unbiotinylated precursor indicates that there is some transient interaction between the precursor–avidin complex and the translocation machinery. The *E. coli* Tat machinery apparently has the capability to differentiate between protein complexes that are fully assembled and those that are not [31,33]. It therefore appears that the thylakoid Tat machinery has retained this capability and is able to recognize that there is something unusual about our precursor–avidin complex and so the machinery rejects this potential translocation substrate. This proofreading mechanism functions after recognition but before commitment to transport. Recent work by Asai and co-workers [34] with a biotinylated version of pOE23 led to results very different to those reported here. With their biotinylated precursor, these investigators were able to form a translocation intermediate in the presence of avidin. At present, we do not know why the two similar precursor constructs behave so differently.

The strong membrane-binding properties of our non-transportable precursor–avidin complex are expected for a translocation intermediate. However, for a transport process characterized by a linear sequence of successive binding events, formation of a stable translocation intermediate should preclude the subsequent transport of a different substrate on the same pathway. As our membrane-bound precursor–avidin complex competitively impeded transport of unbiotinylated precursor rather than block transport completely, the precursor's membrane-bound state was examined further. The data presented here are consistent with a model in which the first step of pOE17 translocation across the thylakoid membrane is binding to the thylakoid membrane surface; the precursor would then encounter the translocation complex through lateral diffusion along the membrane surface. Similar protein–lipid binding interactions involving precursors transported across the *E. coli* inner membrane, the mitochondrial membranes and the chloroplast envelope have been described previously [50–54]. If the precursor binds to the membrane lipids themselves, this interaction is dependent on lipid composition and/or packing structure as the rate of binding to pure lipid vesicles is over one order of magnitude slower than that to the thylakoid membrane (compare Fig. 9C with Fig. 7A). Binding to the membrane lipid itself rather than a receptor complex is expected to be much more difficult to saturate due to its large surface area (and therefore many 'binding sites'). Alternatively, we note that the data presented here do not rule out the possibility that the thylakoid membrane-bound state is achieved through interaction with a membrane protein. A situation in which proteinaceous receptors far outnumber the translocation 'pore' complexes would explain increased concentrations of bound precursor when the import velocity is already saturated (Fig. 3A,B). Consistent with this interpretation, it has recently been estimated that the putative receptor proteins Tha4 and Hcf106 outnumber the translocation pores by about 10 to 1 [22].

The biphasic kinetics observed when thylakoids and pOE17(C)-BioHis are mixed and then immediately illuminated (Fig. 6A) has been observed earlier for full-length wild-type precursors [42,43]. These data indicate that the BioHis tag has a minimal effect, if any, on the import kinetics. The irreversible two-step first-order kinetic model describes a progression from unbound precursor to mature protein through a kinetically distinct intermediate state. The intermediate state is achieved in the absence of energetic input (dark reactions) as revealed in Fig. 7B, whereas reaction completion requires a PMF (light reactions). One interpretation is that the initial lag in the appearance of mature protein when import was initiated immediately after mixing precursor and thylakoids (Figs 6 and 7) is a consequence of the fact that the precursor must first bind to the thylakoid membrane and this binding event is relatively slow (half-time on order of a tens of seconds) under the experimental conditions. Alternatively, the membrane binding event can be fast yet the membrane transport reactions proceed in the dark beyond a later slow kinetic step before transport is arrested by insufficient energy input. We can not at present distinguish between these possibilities.

An intriguing question to arise from this study is the nature of the precursor–membrane interaction. The lack of dissociation in 3 M NaCl (Fig. 8) indicates that the interaction is not ionic. The minimal dissociation by high pH treatment (sodium carbonate) indicates that the binding is not mediated through charged basic residues, in agreement with the NaCl data. The increased dissociation by increasing concentrations of urea (Fig. 8) is more difficult to interpret because it mirrors the precursor folding profile as determined by tryptophan fluorescence (Fig. 4B). It is possible that there exists a hydrophobic patch on the folded precursor mediating the binding to the thylakoid membrane that is lost when the precursor unfolds at high urea concentrations. The more likely explanation, however, is that the hydrophobic region in the LTD interacts hydrophobically with the thylakoid membrane and this interaction is weakened in the presence of urea. We note that all LTDs contain a hydrophobic stretch of 14–22 residues [7,55] and thus urea dissociation may be a characteristic of all Tat precursors. As urea typically dissociates proteins bound by hydrophobic interactions in an environment accessible via an

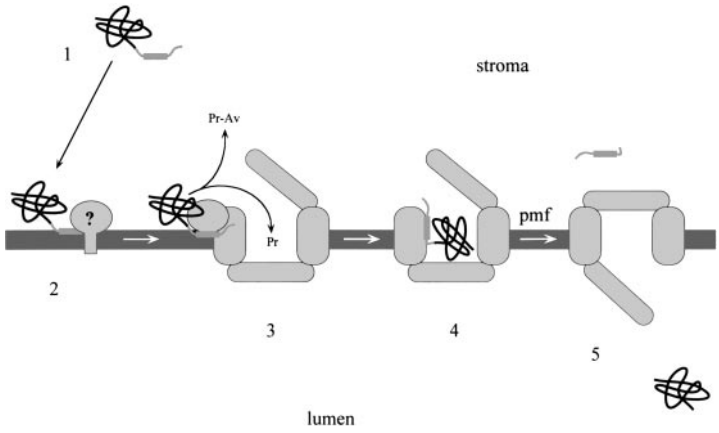

Fig. 10. Schematic of the translocation process catalyzed by the thylakoid Tat machinery. The membrane binding event (1 → 2), shown here as a hydrophobic interaction between presequence and membrane, is followed by LTD binding to the recognition domain on the translocation complex (3). The uncertain involvement of a proteinaceous receptor (e.g. Hcf106 and/or Tha4) in the initial membrane-bound state is denoted by the question mark. At ice temperature, the membrane–presequence interaction is disrupted by urea, yet stable in high salt or high pH buffer. Transfer of the precursor substrate into the pore cavity of the machinery requires dissociation of the presequence from the recognition domain (3 → 4); avidin bound to pOE17(C)-BioHis interferes with this directed movement and the precursor–avidin complex (Pr-Av) is released leading to aborted import. Once the precursor (Pr) is in the pore cavity, the PMF drives transport, releasing the mature protein (black) into the lumen (5). In this scheme, the precursor contains only an LTD; if an STD is present as for pOE17(C)-BioHis, there is simply a longer N-terminal extension. The fate of the presequence is unknown at present, although Fincher and co-workers [60] have observed that an N-terminally attached OE23 mature domain appears in the stroma.

aqueous channel [44,56–58], it can be surmised that the bound LTD binding domain is accessible from an aqueous phase (e.g. the stroma). A scheme summarizing the various steps of transport as discussed here is given in Fig. 10. It is important to point out that the precursor used in these studies contains the STD. While it is quite common to study import of full-length precursor into isolated thylakoids [20,29,30,42,43], the thylakoid membrane interactions of the *in vivo* substrate, the intermediate length precursor, may differ from those identified here for the full-length precursor. Future experiments are planned to address this issue.

While little is understood about the mechanism of transport, a model which requires multiple cycles, such as the multiple cycles of SecA ATP hydrolysis for the Sec machinery, is no longer a necessity in light of the finding that fully folded proteins can be transported by the Tat machinery. For example, a proteinaceous membrane pore that utilizes an 'air-lock'-type mechanism (Fig. 10) to alternate access to stromal and lumenal sides of the membrane and can accommodate a large (e.g. $>$ 100 kDa) folded protein suitably explains both how folded proteins are transported and why there is no detectable concomittant ion leakage [42]. The actual transit time for such a mechanism could in principle be quite short as it involves precursor binding within the 'pore', the opening and closing of gates and precursor dissociation. Such a model, while admittedly speculative, is entirely consistent with the data presented here and elsewhere [29,30,42].

The body of work that has emerged demonstrating that both the bacterial and thylakoid Tat machineries can transport folded proteins and the report here of a membrane-bound, competitive, yet nontransportable substrate quite convincingly portray the Tat machinery as a protein translocating apparatus considerably different to the endoplasmic reticulum, mitochondrial and (cp)Sec machineries, all of which transport proteins linearly in an N-terminal to C-terminal fashion. Consequently, an alternative transport paradigm is required for the Tat machinery. The scheme in Fig. 10 embodies one possible mechanism, although others involving pores or vesicular encapsulation have not been ruled out. Both vesicularization and gated pore mechanisms have been postulated to explain peroxisomal protein import, a translocation system that also accomodates folded and assembled protein complexes [59]. It will be interesting to compare these two translocation systems as their characterization continues.

ACKNOWLEDGEMENTS

This work was supported by National Research Service Award 1-F32-GM18135 from the National Institute of General Medical Sciences (S. M. M.) and US Department of Agriculture Grant 95-37304-2325 (S. M. T.). Special thanks to Melanie Tomczak for guidance on the construction and column purification of thylakoid lipid vesicles, and to Tadeusz Molinski (UC Davis) for use of his CD spectrophotometer. The efforts of Quoc Luu in constructing a pOE23-BioHis precursor and the permission to discuss unpublished attempts to import this precursor are gratefully acknowledged.

REFERENCES

1. Schnell, D.J. (1998) Protein targeting to the thylakoid membrane. *Annu. Rev. Plant Physiol. Plant Mol. Biol.* **49**, 97–126.
2. Cline, K. & Henry, R. (1996) Import and routing of nucleus-encoded chloroplast proteins. *Annu. Rev. Cell Dev. Biol.* **12**, 1–26.
3. Bogsch, E.G., Sargent, F., Stanley, N.R., Berks, B.C., Robinson, C. & Palmer, T. (1998) An essential component of a novel bacterial protein export system with homologues in plastids and mitochondria. *J. Biol. Chem.* **273**, 18003–18006.
4. Sargent, F., Bogsch, E.G., Stanley, N.R., Wexler, M., Robinson, C., Berks, B.C. & Palmer, T. (1998) Overlapping functions of components of a bacterial Sec-independent protein export pathway. *EMBO J.* **17**, 3640–3650.
5. Weiner, J.H., Bilous, P.T., Shaw, G.M., Lubitz, S.P., Frost, L., Thomas, G.H., Cole, J.A. & Turner, R.J. (1998) A novel and ubiquitous system for membrane targeting and secretion of cofactor-containing proteins. *Cell* **93**, 93–101.
6. Brink, S., Bogsch, E.G., Edwards, W.R., Hynds, P.J. & Robinson, C. (1998) Targeting of thylakoid proteins by the pH-driven twin-arginine translocation pathway requires a specific signal in the hydrophobic domain in conjunction with the twin-arginine motif. *FEBS Lett.* **434**, 425–430.
7. Berks, B.C. (1996) A common export pathway for proteins binding complex redox cofactors? *Mol. Microbiol.* **22**, 393–404.
8. Mori, H. & Cline, K. (1998) A signal peptide that directs non-Sec transport in bacteria also directs efficient and exclusive transport on the thylakoid delta pH pathway. *J. Biol. Chem.* **273**, 11405–11408.
9. Duong, F. & Wickner, W. (1997) Distinct catalytic roles of the SecYE, SecG and SecDFyajC subunits of preprotein translocase holoenzyme. *EMBO J.* **16**, 2756–2768.
10. Ernst, F., Hoffschulte, H.K., Thome-Kromer, B., Swidersky, U.E., Werner, P.K. & Müller, M. (1994) Precursor-specific requirements for SecA, SecB and $\Delta\mu_{H+}$ during protein export of *Escherichia coli*. *J. Biol. Chem.* **269**, 12840–12854.
11. Akimaru, J., Matsuyama, S., Tokuda, H. & Mizushima, S. (1991) Reconstitution of a protein translocation system containing purified SecY, SecE, and SecA from *Escherichia coli*. *Proc. Natl Acad. Sci. USA* **88**, 6545–6549.
12. Schiebel, E., Driessen, A.J.M., Hartl, F.-U. & Wickner, W. (1991) $\Delta\mu_{H+}$ and ATP function at different steps of the catalytic cycle of preprotein translocase. *Cell* **64**, 927–939.
13. Wickner, W. & Leonard, M.R. (1996) *Escherichia coli* preprotein translocase. *J. Biol. Chem.* **271**, 29514–29516.
14. Bassilana, M. & Wickner, W. (1993) Purified *Escherichia coli* preprotein translocase catalyzes multiple cycles of precursor protein translocation. *Biochemistry* **32**, 2626–2630.
15. Laidler, V., Chaddock, A.M., Knott, T.G., Walker, D. & Robinson, C. (1995) A SecY homolog in *Arabidopsis thaliana*. *J. Biol. Chem.* **270**, 17664–17667.
16. Voelker, R., Mendel-Hartvig, J. & Barken, A. (1997) Transposon-disruption of a maize nuclear gene, *tha1*, encoding a chloroplast SecA homologue: *in vivo* role of cp-SecA in thylakoid protein targeting. *Genetics* **145**, 467–478.
17. Schuenemann, D., Amin, P., Hartmann, E. & Hoffman, N.E. (1999) Chloroplast SecY is complexed to SecE and involved in the translocation of the 33-kDa but not the 23-kDa subunit of the oxygen-evolving complex. *J. Biol. Chem.* **274**, 12177–12182.
18. Robinson, C., Klösgen, R.B., Herrmann, R.G. & Schackleton, J.B. (1993) Protein translocation across the thylakoid membrane – a tale of two mechanisms. *FEBS Lett.* **325**, 67–69.
19. Klösgen, R.B., Brock, I.W., Herrmann, R.G. & Robinson, C. (1992) Proton gradient-driven import of the 16 kDa oxygen-evolving complex protein as the full precursor protein by isolated thylakoids. *Plant Mol. Biol.* **18**, 1031–1934.
20. Cline, K., Ettinger, W.F. & Theg, S.M. (1992) Protein-specific energy requirements for protein transport across or into thylakoid membranes. *J. Biol. Chem.* **267**, 2688–2696.
21. Settles, A.M., Yonetani, A., Baron, A., Bush, D.R., Cline, K. & Martienssen, R. (1997) Sec-independent protein translocation by the maize hcf106 protein. *Science* **278**, 1467–1470.
22. Mori, H., Summer, E.J., Ma, X. & Cline, K. (1999) Component specificity for the thylakoidal Sec and Delta pH-dependent protein transport pathways. *J. Cell Biol.* **146**, 45–55.
23. Walker, M.B., Roy, L.M., Coleman, E., Voelker, R. & Barkan, A. (1999) The maize *tha4* gene functions in Sec-independent protein transport in chloroplasts and is related to *hcf106*, *tatA* and *tatB*. *J. Cell Biol.* **147**, 267–275.
24. Vestweber, D. & Schatz, G. (1988) A chimeric mitochondrial precursor

protein with internal disulfide bridges blocks import of authentic precursors into mitochondria and allows quantitation of import sites. *J. Cell Biol.* **107**, 2037–2043.
25. Mothes, W., Prehn, S. & Rapoport, T.A. (1994) Systematic probing of the environment of a translocating secretory protein during translocation through the ER membrane. *EMBO J.* **13**, 3973–3982.
26. Behrmann, M., Koch, H.-G., Hengelage, T., Wieseler, B., Hoffschulte, H.K. & Müller, M. (1998) Requirements for the translocation of elongation-arrested ribosome-associated OmpA across the plasma membrane of *Escherichia coli*. *J. Biol. Chem.* **273**, 13898–13904.
27. Joly, J.C. & Wickner, W. (1993) The SecA and SecY subunits of translocase are the nearest neighbors of a translocating preprotein, shielding it from phospholipids. *EMBO J.* **12**, 255–263.
28. Endo, T., Kawakami, M., Goto, A., America, T., Weisbeek, P. & Nakai, M. (1994) Chloroplast protein import: chloroplast envelopes and thylakoids have different abilities to unfold proteins. *Eur. J. Biochem.* **225**, 403–409.
29. Hynds, P.J., Robinson, D. & Robinson, C. (1998) The Sec-independent twin-arginine translocation system can transport both tightly folded and malfolded proteins across the thylakoid membrane. *J. Biol. Chem.* **273**, 34868–34874.
30. Clark, S.A. & Theg, S.M. (1997) A folded protein can be transported across the chloroplast envelope and thylakoid membranes. *Mol. Biol. Cell* **8**, 923–934.
31. Santini, C., Ize, B., Chanal, A., Müller, M., Giordano, G. & Wu, L. (1998) A novel Sec-independent periplasmic protein translocation pathway in *Escherichia coli*. *EMBO J.* **17**, 101–112.
32. Dreusch, A., Bürgisser, D.M., Heizmann, C.W. & Zumft, W.G. (1997) Lack of copper insertion into unprocessed cytoplasmic nitrous oxide reductase generated by an R20D substitution in the arginine consensus motif of the signal peptide. *Biochim. Biophys. Acta* **1319**, 311–318.
33. Rodrigue, A., Chanal, A., Beck, K., Müller, M. & Wu, L.-F. (1999) Co-translocation of a periplasmic enzyme complex by a hitchhiker mechanism through the bacterial Tat pathway. *J. Biol. Chem.* **274**, 13223–13228.
34. Asai, T., Shinoda, Y., Nohara, T., Yoshihisa, T. & Endo, T. (1999) Sec-dependent pathway and pH-dependent pathway do not share a common translocation pore in thylakoid protein transport. *J. Biol. Chem.* **274**, 20075–20078.
35. Schatz, P.J. (1993) Use of peptide libraries to map the substrate specificity of a peptide-modifying enzyme: a 13 residue consensus peptide specifies biotinylation in *Escherichia coli*. *Bio/Technology* **11**, 1138–1143.
36. Sambrook, J., Fritsch, E.F. & Maniatis, T. (1989) *Molecular Cloning: a Laboratory Manual*, 2nd edn. Cold Spring Harbor Laboratory Press, Cold Spring Harbor, New York.
37. Chapman-Smith, A., Turner, D.L., Cronan, J.J.E., Morris, T.W. & Wallace, J.C. (1994) Expression, biotinylation and purification of a biotin-domain peptide from the biotin carboxy carrier protein of *Escherichia coli* acetyl-CoA carboxylase. *Biochem. J.* **302**, 881–887.
38. Cline, K., Werner-Washburne, M., Lubben, T.H. & Keegstra, K. (1985) Precursors to two nuclear-encoded chloroplast proteins bind to the outer envelope membrane before being imported into chloroplasts. *J. Biol. Chem.* **260**, 3691–3696.
39. Cline, K. (1986) Import of proteins into chloroplasts: membrane integration of a thylakoid precursor protein reconstituted in chloroplast lysates. *J. Biol. Chem.* **261**, 14804–14810.
40. Arnon, D.I. (1949) Copper enzymes in isolated chloroplasts: polyphenoloxidase in *Beta vulgaris*. *Plant Physiol.* **24**, 1–15.
41. Creighton, T.E. (1993) *Proteins: Structures and Molecular Properties*, 2nd edn. W. H. Freeman, New York.
42. Teter, S.A. & Theg, S.M. (1998) Energy-transducing thylakoid membranes remain highly impermeable to ions during protein translocation. *Proc. Natl Acad. Sci. USA* **95**, 1590–1594.
43. Brock, I.W., Mills, J.D., Robinson, D. & Robinson, C. (1995) The pH-driven, ATP-independent protein translocation mechanism in the chloroplast thylakoid membrane: kinetics and energetics. *J. Biol. Chem.* **270**, 1657–1662.
44. Gilmore, R. & Blobel, G. (1985) Translocation of secretory proteins across the microsomal membrane occurs through an environment accessible to aqueous perturbants. *Cell* **42**, 497–505.
45. Fujiki, Y., Hubbard, A.L., Fowler, S. & Lazarow, P.B. (1982) Isolation of intracellular membranes by means of sodium carbonate treatment: application to endoplasmic reticulum. *J. Cell Biol.* **93**, 97–102.
46. Webb, M.S. & Green, B.R. (1991) Biochemical and biophysical properties of thylakoid acyl lipids. *Biochim. Biophys. Acta* **1060**, 133–158.
47. Pommier, J., Méjean, V., Giordano, G. & Iobbi-Nivol, C. (1998) TorD, a cytoplasmic chaperone that interacts with the unfolded trimethylamine N-oxide reductase enzyme (TorA) in *Escherichia coli*. *J. Biol. Chem.* **273**, 16615–16620.
48. Wexler, M., Bogsch, E.G., Klösgen, R.B., Palmer, T., Robinson, C. & Berks, B.C. (1998) Targeting signals for a bacterial Sec-independent export system direct plant thylakoid import by the pH pathway. *FEBS Lett.* **431**, 339–342.
49. Creighton, A.M., Hulford, A., Mant, A., Robinson, D. & Robinson, C. (1995) A monomeric, tightly folded stromal intermediate on the ΔpH-dependent thylakoid protein transport pathway. *J. Biol. Chem.* **270**, 1663–1669.
50. McKnight, C.J., Briggs, M.S. & Gierasch, L.M. (1989) Functional and nonfunctional LamB signal sequences can be distinguished by their biophysical properties. *J. Biol. Chem.* **264**, 17293–17297.
51. Hoyt, D.W., Cyr, D.M., Gierasch, L.M. & Douglas, M.G. (1991) Interaction of peptides corresponding to mitochondrial presequences with membranes. *J. Biol. Chem.* **266**, 21693–21699.
52. Pinnaduwage, P. & Bruce, B.D. (1996) *In vitro* interaction between a chloroplast transit peptide and chloroplast outer envelope lipids is sequence-specific and lipid class-dependent. *J. Biol. Chem.* **271**, 32907–32915.
53. van't Hof, R., van Klompenburg, W., Pilon, M., Kozubek, A., de Korte-Kool, G., Demel, R.A., Weisbeek, P.J. & de Kruijff, B. (1993) The transit sequence mediates the specific interaction of the precursor of ferredoxin with chloroplast envelope membrane lipids. *J. Biol. Chem.* **268**, 4037–4042.
54. Theg, S.M. & Geske, F.J. (1992) Biophysical characterization of a transit peptide directing chloroplast protein import. *Biochemistry* **31**, 5053–5060.
55. de Boer, A.D. & Weisbeek, P.J. (1991) Chloroplast protein topogenesis. Import, sorting and assembly. *Biochim. Biophys. Acta* **1071**, 221–253.
56. Sztul, E.S., Chu, T.W., Strauss, A.W. & Rosenberg, L.E. (1989) Translocation of precursor proteins into the mitochondrial matrix occurs through an environment accessible to aqueous perturbants. *J. Cell Sci.* **94**, 695–701.
57. Breyton, C., de Vitry, C. & Popot, J.-L. (1994) Membrane association of cytochrome b_6f subunits: the Rieske iron–sulfur protein from *Chlamydomonas reinhardtii* is an extrinsic protein. *J. Biol. Chem.* **269**, 7597–7602.
58. Pfanner, N., Hartl, F.-U., Guiard, B. & Neupert, W. (1987) Mitochondrial precursor proteins are imported through a hydrophilic membrane environment. *Eur. J. Biochem.* **169**, 289–293.
59. Waterham, H.R. & Cregg, J.M. (1997) Peroxisome biogenesis. *Bioessays* **19**, 57–66.
60. Fincher, V., McCaffery, M. & Cline, K. (1998) Evidence for a loop mechanism of protein transport by the thylakoid delta pH pathway. *FEBS Lett.* **423**, 66–70.